Properties of interfacial transition zones (ITZs) in concrete containing recycled mixed aggregate

Saez del Bosque, I.F.; Zhu, Wenzhong; Howind, Torsten; Matías, A.; Sanchez de Rojas, M.I.; Medina, C

Published in:
Cement & Concrete Composites

DOI:
10.1016/j.cemconcomp.2017.04.011

Published: 01/08/2017

Document Version
Peer reviewed version

Accepted Manuscript

PROPERTIES OF INTERFACIAL TRANSITION ZONES (ITZs) IN CONCRETE CONTAINING RECYCLED MIXED AGGREGATE

I.F. Sáez del Bosque, W. Zhu, T. Howind, A. Matías, M.I. Sánchez de Rojas, C. Medina

PII: S0958-9465(17)30400-6

DOI: 10.1016/j.cemconcomp.2017.04.011

Reference: CECO 2822

To appear in: *Cement and Concrete Composites*

Received Date: 14 March 2016

Revised Date: 15 December 2016

Accepted Date: 25 April 2017

Please cite this article as: I.F. Sáez del Bosque, W. Zhu, T. Howind, A. Matías, M.I. Sánchez de Rojas, C. Medina, PROPERTIES OF INTERFACIAL TRANSITION ZONES (ITZs) IN CONCRETE CONTAINING RECYCLED MIXED AGGREGATE, *Cement and Concrete Composites* (2017), doi: 10.1016/j.cemconcomp.2017.04.011.

PROPERTIES OF INTERFACIAL TRANSITION ZONES (ITZs) IN CONCRETE CONTAINING RECYCLED MIXED AGGREGATE

I.F. Sáez del Bosque[1*], W. Zhu[2], T. Howind[2], A. Matías[1], M.I. Sánchez de Rojas[3], C. Medina[1**]
1.School of Engineering, University of Extremadura, UEX-CSIC Partnering Unit, 10071 - Cáceres, Spain
2. School of Engineering and Computing, University of the West of Scotland, Paisley Campus, Paisley PA1 2BE, United Kingdom
3. Eduardo Torroja Institute for Construction Science, C/ Serrano Galvache, 28033 - Madrid, Spain
Corresponding authors:
**isa.f.saez@gmail.com/ isaezdelu@unex.es*
*** cmedinam@unex.es / cemedmart@yahoo.es*

Abstract

Concretes containing mixed recycled aggregate (RA) have a larger number of coarse aggregate/paste interfacial transition zones (ITZs) than conventional concretes, due to the various component materials present in recycled aggregate. This study investigated the properties of various RA/paste ITZs in concrete using nanoindentation and scanning electron microscopy (SEM) and analysed the possible impact of the properties of the ITZs on the macro-mechanical performance of recycled concrete. It was found that the elastic modulus of the ITZ varies with the type of constituent materials present in recycled aggregate, with ITZs associated with organic components (e.g. wood, plastic and asphalt) exhibiting lower minimum elastic modulus values. The impact of ITZ properties on macro-mechanical properties of concrete depends on the relative content of different constituent materials present in the recycled aggregate and the micro-mechanical properties of the ITZs involved.

***Keywords**: interfacial transition zone, recycled aggregate, elastic modulus, thickness, engineering properties*

1. Introduction

The reuse of construction and demolition waste (C&DW) has become a necessity in modern societies. The aim is to further the efficient use of resources and replace linear with circular economies in which waste materials are repeatedly reused to generate new products or raw materials [1].

At this time, the recycle rate for construction and demolition waste in the European Union varies widely from country to country, ranging from 10 to 90 % [2]. Many recent studies have focused on assessing the effect of using recycled concrete aggregate [3-5] or recycled mixed [6-10] C&DW aggregate on concrete workability, shrinkage, creep, mechanical strength and durability.

The interfacial transition zone (ITZ) between recycled aggregate and paste has been studied less intensely, and moreover, the limited research conducted has focused primarily on its microstructure.

The microstructure of the ITZ in concrete varies widely from what is found in cement paste (greater porosity, precipitation of long portlandite crystals and greater ettringite content) [11]. It is regarded as the third constituent phase in concrete, along with coarse aggregate and cement paste [12]. A full understanding of this region would afford a scientific explanation for the macroscopic performance of recycled concrete given: a) the effect of the zone on concrete strength and permeability; and b) the possible of impact of a larger number of recycled aggregate/paste ITZs present in new eco-efficient concretes [12].

While ITZ microstructure in cementitious materials may be analysed with a number of instrumental techniques (including electron or atomic force microscopy and nanoindentation), scanning or back-scattered electron microscopy (SEM/BSE) has traditionally been the research community's method of choice. With the development and improvement of nanoindentation in recent decades, information is now accessible on the modulus of elasticity in the ITZ and its width/thickness, properties that could not be determined with the techniques traditionally applied [11, 13].

Limited research published using nanoindentation to study ITZ nano-mechanical properties has mainly analysed the ITZ between recycled concrete aggregate and cement paste [2, 13-15]. To the best of our knowledge, no studies have been published in international journals on the micro-mechanical properties of the ITZs between the paste and each constituent (such as asphalt, brick, glass, wood or plastic) found in mixed recycled C&DW aggregate. This is a question of practical significance, inasmuch as in some European Union countries such as Spain, 63 % of the volume of recycled aggregate is mixed, i.e., with less than 95 wt% of crushed concrete and unbound aggregate and over 5 wt% of clay-based material, asphalt and floating particles (primarily glass, wood and plastic) [8].

This study is the first to explore the thickness and elastic modulus of the ITZs between the various components of mixed recycled aggregate and paste in recycled concretes with over 50% mixed recycled aggregate. To that end, the micro-mechanical properties of the ITZs associated with the various constituents present in the mixed recycled aggregate (i.e. concrete,

brick or clay-based material, asphalt, plastic, glass and wood) were determined. The width/thickness of the ITZs determined using SEM and nanoindentation techniques were compared. The likely impact of such ITZs on macro-mechanical properties of concrete was also discussed.

2. Materials and experimental

2.1. Materials

The natural aggregate used had a coarse fraction (gravel) measuring 4-20 mm and a fines fraction (sand) with a grain size of under 4 mm. The majority oxides in these aggregates, SiO_2 and Al_2O_3, accounted for 67 wt% of the total, while the remainder comprised Fe_2O_3, Na_2O and CaO. Although the predominant mineralogical phase was quartz, smaller proportions of feldspars and phyllosilicates were also present [7, 8].

The mixed recycled aggregate (RA) used, with a particle size ranging from 4 to 20 mm, comprised primarily stone-like (Rc > Ru > Ra > Rb) but also other minority materials (such as glass, plastic, metal and wood) (Figure 1).

Figure 1. Composition of recycled mixed aggregate

Table 1 lists the physical and mechanical properties of the coarse aggregate used in this study. The grading modulus obtained for the coarse aggregate fell within the 5.5–8.5 interval ordinarily used in concrete manufacture [16], an indication that the mean particle size was similar to the value observed in conventional aggregate.

Table 1. Physical and mechanical properties of coarse aggregates

The recycled aggregate exhibited higher crushing value and water absorption and lower density than the natural material. These findings were directly associated with the intrinsic properties of the main constituents of the recycled mixed aggregate as described by other authors [17-20].

SiO_2, Al_2O_3 and Fe_2O accounted for 65 wt% of the total chemical composition of the recycled aggregate, with other minority oxides and trace elements such as Ba, Zr, Cl and Cr.

The mineralogical composition of the bulk samples was determined with random powder X-ray diffraction (XRD) on a BRUKER Theta-Theta D8 Advance diffractometer fitted with a 2.2 kW Cu anode, operating in the absence of a monochromator. Quartz, the majority mineralogical phase in this mixed aggregate, was found along with lesser proportions of feldspars (albite, orthoclase and sanidine), hematite, magnetite and calcite [7].

The concretes were prepared using CEM I 52.5 R portland cement containing at least 95 % clinker, as specified in European standard EN 197-1 [21].

2.2. Concrete mixes used

The recycled mixed aggregate was processed manually to produce further three sub-types of the recycled mixed aggregate, i.e. i) by removing all the floating particles (FL); ii) by removing all the brick or clay-based materials (Rb); iii) by removing all the asphalt particles (Ra). This facilitates the isolation of various components for studying their possible effects on concrete properties. The four types of concretes prepared were using: 50 % recycled mixed aggregate (RC50); 50 % recycled mixed aggregate without floating particles (RC50-FL); 50 % recycled mixed aggregate without brick or clay-based particles (RC50-Rb); and 50 % recycled mixed aggregate without asphalt particles (RC50-Ra).

The concretes, designed using the British Department of Environment Method [22], had a characteristic strength of 30 MPa and an effective water/cement ratio of 0.65. The amount of mixing water added was adjusted to natural and mixed recycled aggregate absorptivity.

The concrete was mixed and cured as specified in European standard EN 12390-2 [23] and moulded into 100x100x100 mm specimens (6 cubes/concrete type) for testing. Concrete batching particulars and slump and 28 day bulk density values are given in Tables 2 and 3, respectively.

Table 2. Concrete mix proportions

Table 3. Physical properties of the concretes

The empirical formula set out in ACI 318-08 [24], which defines the elastic modulus in terms of concrete 28 day compressive strength and bulk density, was used to obtain this property .

2.3. Sample preparation for nanoindentation test

The reliability of results obtained from nanoindentation highly depends on the surface quality of the sample to be tested. Thus sample preparation is a very important part of the nanoindentation studies on cementitious materials [25]. The heterogeneity of the material demands a complex sample preparation procedure.

After 28 days curing in a water tank, the centre piece of each of the 100×100×100 mm^3 cubes was extracted using a diamond saw. Each center piece was later cut into small samples of the size about 15x15x10 mm. For the further preparation and ease sample handling in the polishing

machine all specimens were embedded in resin disks (Ø 30 mm) followed by a vacuum impregnation with an epoxy resin with an elastic modulus of around 3-4 GPa. The resin impregnation was required to support and prevent the loss of the weaker phases in the ITZ and the cement paste during the specimen preparation. To obtain the final test specimens for nanoindentation subsequent grinding and polishing steps were performed, finishing the polishing with ¼ µm diamond particle spray (figure 2). Throughout the preparation process only alcohol or oil-based polishing sprays and lubricants were used to avoid further cement hydration and possible dissolution of hydrate phases [26].

Figure 2. Indentation specimens: a) recycled concrete aggregate (Rc)/paste; b) brick or clay-based material (Rb)/paste; c) asphalt (Ra)/paste; d) glass (GL)/paste; e) plastic (PL)/paste; f) wood (W)/paste

2.4. Nanoindentation testing

Although nanoindentation is used by many researches in the world to determine micro-mechanical properties of various materials we recall briefly its operational principles. Indentation starts by establishing contact between the indenter tip of known geometry and mechanical properties and the material sample of which we want to determine the mechanical properties. When in contact an increasing load is applied to the indenter causing the tip to penetrate the investigated surface. After reaching a predefined maximum the load is normally kept at this level for a short period (hold segment) to account for creep before the load is eventually withdrawn from the indenter. The elastic recovery of the deformed material results in a reduction of the penetration depth [27, 28]. During the duration of the whole indentation experiment the changes in load (P) and depth (h) are continuously monitored. A typical outcome of such testing is an indentation load vs. displacement (indentation depth) hysteresis curve (figure 3).

Figure 3. Indentation load vs. displacement curve obtained from nanoindentation/instrumented indentation testing

The determination of the elastic recovery through analysis of the unloading data in accordance to a model for the elastic contact problem enables to calculate the reduced modulus, *Er*, and subsequently the Young's modulus, *E*, of the probed material. Details of the theoretical background and methodology for determining the modulus of elasticity from instrumented

indentation testing have been reviewed and discussed by Oliver and Pharr thus leading to the following equations 1 and 2 [29-31]:

$$S = \frac{dP}{dh} = \frac{2}{\sqrt{\pi}} E_r \sqrt{A} \qquad (Equation\ 1)$$

$$\frac{1}{E_r} = \frac{(1 - v^2)}{E} + \frac{(1 - v_i^2)}{E_i} \qquad (Equation\ 2)$$

where *S=dP/dh*, is the slope of the upper portion of the unloading curve during the initial stages of unloading (also called contact stiffness). In Eqs. (1) and (2) *Er* stands for the reduced modulus, *A* is the projected contact area of the indenter tip, and *E* is the Young´s modulus and *v* is Poisson's ratio of the tested materials. Finally, *Ei* and *vi* represent the material parameter of the indenter type (e.g. diamond, *Ei* = 1141 GPa and *vi* = 0.07).

The nanoindentation experiments in this study were performed using an Agilent G200 Nano Indenter® fitted with a Berkovich indenter tip.

To study the ITZ properties, grids of indentation testing points with varying distances to the actual aggregate-paste interface were selected. The spacing between the indentation test points used were usually 15 µm or 20 µm to cover a sufficient area and also to avoid possible overlapping of the test areas. Nanoindentation testing with a maximum load of 2 mN (corresponding to an average indentation depth of 300 nm in most cases) was carried out at each grid point. The perpendicular distance of each indentation point to the actual aggregate – paste interface was measured using an image analysing and the AutoCAD® 2012 tool.

Some selected indentation areas are shown in the BSE images of the ITZ between different aggregates/paste in figure 4. The indentation areas are contained within the rectangles outlined in the figures; the number, which always begins from 1, refers to the sequence of the indentation tests carried out in each chosen indented area, which facilitate the measurement of the distance to ITZ for each test point.

Figure 4. Area indented in recycled aggregate constituent/paste ITZ a) 15x15 µm; y b) 20x20 µm

Validation of test results after the indentation testing was performed for each point to identify abnormal or discontinuous indentation test curves, high surface roughness, large voids or cracking. When such imperfections were detected, which was only rarely (<2% of the total), the respective data were excluded in further data analysis. The total number of valid test points

obtained and used is provided in table 4, covering the various aggregates, ITZs and the bulk paste.

Table 4. Number of indentation tests performed for each constituent type

2.5. Other techniques

The distribution of Ca and Si in the ITZs between the coarse aggregate constituents (recycled concrete aggregate, asphalt, brick, glass, wood and plastic) and the paste was explored on a HITACHI S-4800 scanning electron microscope fitted with a tungsten-source energy dispersive X-ray analyser and a silicon detector. The flat surfaces of the epoxy-coated, precision-sawed samples were carefully polished prior to analysing their microstructure with backscattering electron (BSE) microscopy.

3. Results and discussion

3.1. Aggregate characterisation

Figure 5 shows the elastic modulus for the various components of the recycled mixed aggregate ranged, which indicates that the E values varies from 4.73 GPa (for wood) to 86.17 GPa (for glass). These values were much lower than the 100-120 GPa observed in natural granite aggregate [32]. Such large differences were due to the variable nature of the component materials, present in the recycled aggregate.

Figure 5. Nanoindentation-determined elastic modulus of recycled aggregate components

The variation of E modulus observed within rock materials were mainly due to the differents mineralogical compositions, as well as porosity and cracks present, as reported by Zhu et al. [27] and Ahmed [33].

The E value obtained for the old cement paste in the recycled concrete aggregate lay within the characteristic values (16-24 GPa) reported by Xiao et al. [14] for paste bound to recycled concrete aggregate. That value varied somewhat depending on starting concrete w/c ratio, characteristic strength and other properties.

The E value for the brick material was similar to the modulus reported by Nezerka et al. [34] (≈33 GPa) for this type of material and lower than the values reported for other clay-based materials such as sanitary ware [25].

The elastic modulus recorded for the asphalt material was also in the range of E values (11-53 GPa) observed for this type of material by previous authors [35-37] analysing the properties of the ITZ between aggregate and bituminous binder.

The values for glass likewise lay within the range for this material (E>50 GPa) reported by Mohajeri et al. [35] and Zhao et al. [38].

The findings for plastic were very close to the 5.8 and 7.5 GPa reported by Huang et al. [39] for polycarbonate and polystyrene, respectively.

Lastly, due its anisotropy, the mechanical and elastic properties of wood vary depending on the direction of the load relative to the fibre. The value found here was within the range for the transverse elastic modulus (6.5-3.0 GPa) and much lower than the longitudinal modulus; Bourmaud and Baley [40] reported analogous results.

3.2. Nanoindentation-based characterisation of the ITZ between aggregate and paste

Table 5 presents the nanoindentation results of the elastic modulus in the ITZs between the various RA constituents and the cement paste. The pattern of the E values across the ITZs was similar in all the constituents analysed and concurred with earlier reports on natural [25, 29, 32], recycled crushed concrete [2, 13-15] and clay-based (sanitary ware and bricks) aggregate [2, 25].

Table 5. Elastic modulus (GPa) for recycled aggregate constituents by distance from the aggregate surface

The results in Table 5 reveal the presence of three distinct regions starting and ending at different distances from the interface depending on the constituent. In the area closest to the surface (10-35 μm), the modulus declined to a minimum value that ranged from 13.55 to 22.52 GPa (Table 5). It subsequently rose in the 15-55 μm region and flattened at around 25.94-28.66 GPa at distances between 35 and 60 μm. The value found at the points adjacent to or less than 10 μm from the aggregate surface was affected by that proximity [29] and the perpendicular growth of portlandite plates on the aggregate periphery [41, 42].

The minimum E values of the ITZs (bold in Table 5) reveal that it was the lowest (11.99 GPa) for the plastic/paste, followed by the glass/paste (14.13 GPa), wood/paste (15.07 GPa), asphalt/paste (16.72 GPa) and brick/paste (19.27 GPa) ITZs. These values were 46.7, 37.3, 33.1, 25.6 and 14.4 % lower, respectively, than the modulus (22.52 GPa) observed for the

recycled concrete aggregate/paste ITZ. Earlier papers [43, 44] attributed the weaker bonds between cement and materials such as asphalt, wood and plastic to the organic nature of the latter.

Such behaviour is also related to the surface texture of each component. Materials with smooth surfaces (glass, plastic) exhibit a lower elastic modulus than observed for rough-textured products, including asphalt, fired clay products and concrete aggregate.

The higher minimum E values for the ITZs between the paste and both the recycled concrete and brick could be due to possible pozzolanic reaction [45-47]. The resulting hydrate phases (C-S-H gels and aluminosilicates) would increase binding and reduce porosity in this region [32, 48] thereby improving its micro-mechanical properties. This effect was shown by other authors [14, 15] who pre-treated the recycled aggregate with additions such as fly ash or nanosilica. Moreover, the anhydrous cement particles present in recycled concrete aggregate may react with water to generate further hydration products.

Figure 6 shows the minimum and mean modulus of elasticity in the ITZ between the constituents of the recycled mixed aggregate and the paste and the mean modulus for the paste. The mean aggregate/component ITZ was higher for the stone-like components (clay-based materials and concrete) and asphalt than for the others (wood, plastic and glass). The elastic modulus in the recycled concrete/, clay-based material/, asphalt/, glass/, wood/ and plastic/paste ITZs were respectively 94.1, 83.4, 83.3, 76.1, 72.6 and 71.0 % of the value for the paste. Those percentages were consistent with the hypothesis that the elastic modulus in the ITZ is lower than in the paste (by 15-30 % in natural aggregate [49, 50]).

Figure 6. Minimum and mean elastic modulus (GPa) in the interfacial transition zone (ITZ) and mean value in paste

As expected, the mean values for the bulk paste were very similar irrespective of the type of constituent analysed and lay within the range (7-34 GPa) characteristic of cement hydration products (C-S-H gels) [13].

Figure 7 shows that the thickness of the ITZ between the recycled aggregate constituents and the paste varied with the type of constituent materials. The ITZs for some of the components (recycled concrete aggregate, wood and asphalt) were thicker than the 10-50 μm reported for

natural aggregate/paste ITZs [25, 51, 52]. Glass/paste and plastic/paste ITZ thickness values lay within the aforementioned range.

Figure 7. Nanoindentation-determined thickness of the recycled aggregate constituent/paste ITZ

The ITZ between brick and the paste was thicker than the 30 μm reported by Medina et al. [25] for the clay-based sanitary ware/paste zone, due primarily to the differences between the density and porosity of the two types of aggregate. The thickness recorded for the recycled concrete aggregate/paste ITZ was in agreement with the 55-65 μm reported by other authors [14, 15, 53] studying recycled concrete.

3.3. SEM-based characterisation of the ITZs

The results of SEM-based characterisation of the ITZs between the recycled aggregate constituents and the cement paste are presented in Figure 8.

Figure 8. Microstructural analysis and Ca and Si mapping in ITZs: a) recycled concrete/paste; b) brick/paste; c) asphalt /paste; d) plastic/paste; e) glass/paste; f) wood/paste

These micrographs appear to show a more visible distinctive region in the plastic/, glass/ and wood/paste ITZs, which are possibly due to the weak affinity/bonding between these constituents and the cementitious matrix, and also poor particle packing of cement particles into an area adjacent to a relatively large flat surface of these materials. These observations were consistent with the nanoindentation findings in which the lowest minimum elastic modulus values were obtained for ITZs with plastic, glass and wood materials (see Table 5).

Also, the recycled concrete and brick materials, seem to, adhere more closely to the matrix, exhibiting a more compact and continuous interface than that between the asphalt and the paste due to the weak organic material-cement bonding.

Figure 8 also shows that calcium (Ca) and silicon (Si) were both evenly distributed across the ITZ. A minor rise in Ca concentration was observed in the areas nearest the aggregate, particularly around the recycled concrete, asphalt, glass and wood. These findings were consistent with the EDX analysis (see Table 6). The Si-high regions visible in the cementitious matrix denote the presence of the fines (sand) used to prepare the recycled concrete.

Table 6 lists the variations in the Ca/Si ratio in the ITZs between the recycled aggregate constituents and the paste. The values gradually declined as the distance from the interface

grew, flattening at around 1.73-1.76, which lies within the range (1.2 - 2.3) proposed by Hewlett [54] for calcium silicate hydrates (C-S-H gel).

Lastly, the data show that the width or thickness of the coarse aggregate/paste ITZ varied with the different recycled aggregate constituents, from 40 μm for glass/paste to 80 μm for asphalt/paste.

The width/thickness values of the ITZs obtained using the SEM-based technique were found to be slightly greater than those determined using the nanoindentation-based methods (see Figure 7). However, both techniques appeared to deliver the same pattern as for the different constituent.

3.4. Concrete macro-properties

The mechanical strength and elastic modulus for the concretes prepared using 50 % recycled aggregates are shown in Figure 9, which reveals the possible effect of the different constituents of the recycled aggregate on concrete performance. The removal of floating particles (primarily wood) did not lead to a significant difference in strength of the concrete, likely due to the fact that only less than 2% floating particles were present in the recycled aggregate. The removal of asphalt (RC50-Ra) and brick (RC50-Rb) particles from the recycled aggregate resulted in an increase of compressive strength of concrete by 9.2% and 4.7 % respectively compared to the concrete using the all-in recycled aggregate (RC50). Similarly, the the increase of elastic modulus was moderate, by 5.2% and 3.7% respecitively for the two concrete mixes.

Figure 9. Macro-properties of 28-day concrete

The better mechanical performance observed could be attributable to the effect of the constituents (brick, asphalt, floating particles) on the intrinsic properties of the recycled aggregate [7, 8], their content in the recycled aggregate and the ITZ properties. In terms of properties of the ITZs, the minimum elastic modulus value of the ITZ appears to be of particular significance. This is in good agreement with previous findings reported by Medina et al. [25] in studying recycled aggregate derived from sanitary ware waste/paste ITZ in recycled concretes. Lee and Park [51], and Taqa et al. [49], also suggested that the elastic modulus of concrete was impacted more heavily by the mean value of the elastic modulus in the coarse aggregate/paste ITZ.

4. Conclusions

The following conclusions may be drawn from the findings reported and discussed above:

- The elastic modulus of the ITZ varies with the type of constituent materials present in recycled aggregate, with ITZs associated with organic components (e.g. wood, plastic and asphalt) exhibiting lower minimum elastic modulus values.
- The thickness of the asphalt/, wood/ and recycled concrete aggregate/paste ITZs are: 65 μm, 60μm and 55 μm, respectively. These values are higher than the natural aggregate/paste interfacial transition zone, which normally ranges from 10-50 μm.
- Using electron microscopy and EDX microanalysis appeared to deliver larger ITZ thicknesses than using nanoindentation techniques.
- The properties of the ITZs could have a significant impact on the macro mechanical properties of concrete. However, the degree of influence depends on the relative content of different constituent materials present in the recycled aggregate and the micro-mechanical properties of the ITZs involved.
- Nanoindentation is an indispensable tool for studying and assessing the effect of new materials (recycled aggregate) on the micro-mechanical properties of the ITZ and the macro-mechanical properties of future recycled aggregate concretes.
- Every effort should be made when processing recycled aggregate to reduce the wood, plastic, glass and asphalt content in the end product as far as possible, due to the weak bonding between these components and cementitious matrices.

Acknowledgements

This study was funded by the Spanish Ministry of Science and Innovation under projects BIA 2013-48876-C3-1-R and BIA 2013-48876-C3-2-R, as well as by the Government of Extremadura and the European Regional Development Fund (ERDF) under grant GR 15064 awarded to the MATERIA research group. The experimental research for this study was conducted in conjunction with the University of the West of Scotland during the first and last authors' participation in a visiting scholar exchange.

References

[1] Comission E. Communication from the commission to the european parliament, the council, the european economic and social committee and the committee of the regions. Towards a circular economy: A zero waste programme for Europe. http://ec.europa.eu/environment

/circular-economy/pdf/circular-economy-communication.pdf [Access date: 2/11/2015] 2014. p. 14.

[2] Sidorova A, Vazquez-Ramonich E, Barra-Bizinotto M, Josep Roa-Rovira J, Jimenez-Pique E. Study of the recycled aggregates nature's influence on the aggregate-cement paste interface and ITZ. Construction and Building Materials. 2014;68:677-84.

[3] Thomas C, Setién J, Polanco JA, Alaejos P, Sánchez de Juan M. Durability of recycled aggregate concrete. Construction and Building Materials. 2013;40:1054-65.

[4] Duan ZH, Poon CS. Properties of recycled aggregate concrete made with recycled aggregates with different amounts of old adhered mortars. Materials & Design. 2014;58:19-29.

[5] Poon CS, Chan D. The use of recycled aggregate in concrete in Hong Kong. Resources Conservation and Recycling. 2007;50:293-305.

[6] Mas B, Cladera A, Bestard J, Muntaner D, López CE, Piña S et al. Concrete with mixed recycled aggregates: Influence of the type of cement. Construction and Building Materials. 2012;34:430-41.

[7] Medina C, Zhu W, Howind T, Frías M, Sánchez de Rojas MI. Effect of the constituents (bituminous matter, clay materials, floating particles and fines) of construction and demolition waste on the properties of recycled concretes. Construction and Building Materials. 2015;79:22-33.

[8] Medina C, Zhu W, Howind T, Sánchez de Rojas MI, Frías M. Influence of mixed recycled aggregate on the physical – mechanical properties of recycled concrete. Journal of Cleaner Production. 2014;68:216-25.

[9] Medina C, Sánchez de Rojas MI, Frías M. Properties of recycled ceramic aggregate concretes: Water resistance. Cement and Concrete Composites. 2013;40:21-9.

[10] Medina C, Frías M, Sánchez de Rojas MI, Thomas C, Polanco JA. Gas permeability in concrete containing recycled ceramic sanitary ware aggregate. Construction and Building Materials. 2012;37:597-605.

[11] Xie Y, Corr DJ, Jin F, Zhou H, Shah SP. Experimental study of the interfacial transition zone (ITZ) of model rock-filled concrete (RFC). Cement & Concrete Composites. 2015;55:223-31.

[12] Jin L, Zhang R, Du X, Li Y. Multi-scale analytical theory of the diffusivity of concrete subjected to mechanical stress. Construction and Building Materials. 2015;95:171-85.

[13] Li W, Xiao J, Sun Z, Kawashima S, Shah SP. Interfacial transition zones in recycled aggregate concrete with different mixing approaches. Construction and Building Materials. 2012;35:1045-55.

[14] Xiao J, Li W, Sun Z, Lange DA, Shah SP. Properties of interfacial transition zones in recycled aggregate concrete tested by nanoindentation. Cement & Concrete Composites. 2013;37:276-92.

[15] Zhang H, Zhao Y, Meng T, Shah SP. The modification effects of a nano-silica slurry on microstructure, strength, and strain development of recycled aggregate concrete applied in an enlarged structural test. Construction and Building Materials. 2015;95:721-35.

[16] ACI. ACI 221R-96: Guide for use of normal weight and heavyweight aggregates in concrete. United States: American Concrete Institute Publications; 2001.

[17] Mas B, Cladera A, Olmo Td, Pitarch F. Influence of the amount of mixed recycled aggregates on the properties of concrete for non-structural use. Construction and Building Materials. 2012;27:612-22.

[18] Agrela F, Sánchez de Juan M, Ayuso J, Geraldes VL, Jiménez JR. Limiting properties in the characterisation of mixed recycled aggregates for use in the manufacture of concrete. Construction and Building Materials. 2011;25:3950-5.

[19] de Juan MS, Gutierrez PA. Study on the influence of attached mortar content on the properties of recycled concrete aggregate. Construction and Building Materials. 2009;23:872-7.

[20] Medina C, Sánchez de Rojas MI, Frías M. Reuse of sanitary ceramic wastes as coarse aggregate in eco-efficient concretes. Cement and Concrete Composites. 2012;34:48-54.

[21] European Standard. EN 197-1:2011. Cement - Part 1: Composition, specifications and conformity criteria for common cements.

[22] Teychenné DC, Franklin RE, Erntroy HC. Design of normal concrete mixes. Second Edition ed. Garston , Watford: IHS BRE Press; 2010.

[23] European Standard. EN 12390-2:2009. Testing hardened concrete - Part 2: Making and curing specimens for strength tests.

[24] ACI Comittee 318. 318-08: Building Code Requirements for Structural Concrete and Commentary. Detroit: American Concrete Institute; 2008.

[25] Medina C, Zhu W, Howind T, Sánchez de Rojas MI, Frías M. Influence of interfacial transition zone on engineering properties of the concrete manufactured with recycled ceramic aggregate. Journal of Civil Engineering and Management. 2015;21:83-93.

[26] Howind T. Micromechanical properties of cement-based materials. Paisley - Scotland (United Kingdom): University of the West of Sctoland; 2014.

[27] Zhu W, Hughes J. J., Bicanic N. C., Pearce, J. Nanoindentation mapping of mechanical properties of cement paste and natural rocks, Materials Characterization. 2007; 58,1189-1198.

[28] Zhu W., Bartos P. J. M. Application of depth-sensing microindentation testing to study of interfacial transition zone in reinforced concrete, Cement and Concrete Research. 2000; 30, 1299-1304.

[29] Zhu W, Sonebi M, Bartos PJM. Bond and interfacial properties of reinforcement in self-compacting concrete. Materials and Structures. 2004;37:442-8.

[30] Oliver W. C., Pharr G. M. Measurement of hardness and elastic modulus by instrumented indentation: Advances in understanding and refinements to methodology, Journal of Materials Research. 2004;19, 3-20.

[31] Oliver W. C., Pharr G. M. An improved technique for determining hardness and elastic-modulus using load and displacement sensing indentation experiments, Journal of Materials Research. 1992; 7, 1564-1583.

[32] Sakulich AR, Li VC. Nanoscale characterization of engineered cementitious composites (ECC). Cement and Concrete Research. 2011;41:169-75.

[33] Ahmed SFU. Existence of Dividing Strength in Concrete Containing Recycled Coarse Aggregate. Journal of Materials in Civil Engineering. 2014;26:784-8.

[34] Nezerka V, Nemecek J, Slizkova Z, Tesarek P. Investigation of crushed brick-matrix interface in lime-based ancient mortar by microscopy and nanoindentation. Cement & Concrete Composites. 2015;55:122-8.

[35] Mohajeri M, Molenaar AAA, Van de Ven MFC. Experimental study into the fundamental understanding of blending between reclaimed bituminous matter binder and virgin bitumen

using nanoindentation and nano-computed tomography. Road Materials and Pavement Design. 2014;15:372-84.

[36] Khorasani S, Masad E, Kassem E, Abu Al-Rub RK. Nano-Mechanical Characterization of Mastic, Aggregate, and Interfacial Zone in Bituminous matter Composites. Journal of Testing and Evaluation. 2013;41:924-32.

[37] Stangl K, Jaeger A, Lackner R. Microstructure-based identification of bitumen performance. Road Materials and Pavement Design. 2006;7:111-42.

[38] Zhao Q, Guerette M, Huang L. Nanoindentation and Brillouin light scattering studies of elastic modulus of sodium silicate glasses. Journal of Non-Crystalline Solids. 2012;358:652-7.

[39] Huang C-C, Wei M-K, Harmon JP, Lee S. Nanoindentation creep in polycarbonate and syndiotactic polystyrene. Journal of Materials Research. 2012;27:2746-51.

[40] Bourmaud A, Baley C. Nanoindentation contribution to mechanical characterization of vegetal fibers. Composites Part B-Engineering. 2012;43:2861-6.

[41] Neville AM. Properties of concrete. 1st ed. Harlow (New York): Longman Scientific & Technical John Wiley & Sons; 2008.

[42] Kong DY, Lei T, Zheng JJ, Ma CC, Jiang J. Effect and mechanism of surface-coating pozzalanics materials around aggregate on properties and ITZ microstructure of recycled aggregate concrete. Construction and Building Materials. 2010;24:701-8.

[43] Huang B, Shu X, Burdette EG. Mechanical properties of concrete containing recycled bituminous matter pavements. Magazine of Concrete Research. 2006;58:313-20.

[44] Etxeberria M, Vazquez E, Mari A. Microstructure analysis of hardened recycled aggregate concrete. Magazine of Concrete Research. 2006;58:683-90.

[45] Asensio E, Medina C, Sanchez de Rojas MI, Frias M. Blended cements based on C&DW: its influence in the pozzolanicity. Construction Materials and Structures. 2014:370-7.

[46] Medina C, Banfill PFG, Sánchez de Rojas MI, Frías M. Rheological and calorimetric behaviour of cements blended with containing ceramic sanitary ware and construction/demolition waste. Construction and Building Materials. 2013;40:822-31.

[47] Sánchez de Rojas MI, Marin F, Rivera J, Frias M. Morphology and properties in blended cements with ceramic wastes as a pozzolanic material. Journal of the American Ceramic Society. 2006;89:3701-5.

[48] Li J, Xiao H, Zhou Y. Influence of coating recycled aggregate surface with pozzolanic powder on properties of recycled aggregate concrete. Construction and Building Materials. 2009;23:1287-91.

[49] Abu Taqa AG, Abu Al-Rub RK, Senouci A, Al-Nuaimi N, Bani-Hani KA. The Effect of Interfacial Transition Zone Properties on the Elastic Properties of Cementitious Nanocomposite Materials. Journal of Nanomaterials. 2015;2015:13.

[50] Mondal P, Shah SP, Marks LD. Nanomechanical Properties of Interfacial Transition Zone in Concrete. Nanotechnology in Construction 3, Proceedings. 2009:315-20.

[51] Lee KM, Park JH. A numerical model for elastic modulus of concrete considering interfacial transition zone. Cement and Concrete Research. 2008;38:396-402.

[52] Zheng JJ, Li CQ, Zhou XZ. Thickness of interfacial transition zone and cement content profiles around aggregates. Magazine of Concrete Research. 2005;57:397-406.

[53] Xiao J, Li W, Corr DJ, Shah SP. Effects of interfacial transition zones on the stress-strain behavior of modeled recycled aggregate concrete. Cement and Concrete Research. 2013;52:82-99.

[54] Hewlett PC. Lea´s Chemistry of Cement and Concrete. Fourth Edition ed. London, 1998.

Table 1.Physical and mechanical properties of coarse aggregates

Characteristic	Gravel	Recycled mixed aggregate
Maximum size (mm)	20	20
Grading modulus	5.66	5.77
Particle density on saturated and surface - dried base (kg/dm^3)	2.66	2.54
Water absorption for 24 h (wt. %)	2.66	4.49
Crushing value (wt.%)	16.28	19.72

Table 2.Concrete mix proportions

Concrete	Material (kg/m^3)						
	Sand	Gravel	Recycled aggregate	Cement	Water	$(w/c)_{effective}$ *	$(w/c)_{apparent}$ **
RC-50	941.72	510.10	514.84	323.08	228.57	0.65	0.71
RCF-50	941.72	510.10	514.84	323.08	229.36	0.65	0.71
RC50-AS	941.72	510.10	514.84	323.08	228.76	0.65	0.71
RC50-BR	941.72	510.10	514.84	323.08	228.37	0.65	0.71

Note. * $(w/c)_{effective}$: water used to hydrate the cement
** $(w/c)_{apparent}$: aggregate water absorptivity + water used to hydrate the cement

Table 3.Physical properties of the concretes

Physical property	Slump (mm)	28 day bulk density (kg/m^3)
RC50	30	2320
RC50-FL	30	2335
RC50-Ra	35	2330
RC50-Rb	40	2340

Table 4.Number of indentation tests performed for each constituent type

Constituent type	Number of indentation tests		
	ITZ	Paste	Inner side
Recycled concrete aggregate	96	47	34
Brick or Clay-based materials	51	43	34
Asphalt	50	39	23
Glass	59	49	27
Plastic	68	46	45
Wood	57	47	60

Table 5.Elastic modulus (GPa) for recycled aggregate constituents by distance from the aggregate surface

Distance from interface (μm)	Elastic modulus (GPa)					
	Recycled mixed aggregate constituent					
	Rc	Rb	Ra	GL	PL	W
0.00	44.95±6.94	39.10±8.93	38.11±4.61	81.98±4.71	41.10±3.25	37.48±2.42
5.00	34.19±5.68	33.99±1.33	25.28±5.54	46.80±4.63	23.98±3.93	28.91±3.88
10.00	26.20±3.37	**19.27±3.98**	23.80±4.34	**14.13±3.91**	20.61±2.29	15.33±2.18
15.00	27.25±1.23	20.99±0.40	23.03±3.62	23.62±1.81	11.99±1.99	17.45±1.76
20.00	27.60±1.88	23.82±3.21	23.55±3.40	25.01±2.88	20.19±2.03	**15.07±1.51**
25.00	24.11±3.27	24.88±3.80	**16.72±3.85**	24.46±2.14	20.59±1.44	18.68±2.78
30.00	24.60±2.92	23.95±0.62	21.19±2.20	26.94±2.15	**13.55±2.71**	17.55±0.98
35.00	**22.52±3.15**	24.53±0.67	22.85±0.66	30.65±2.88	21.28±3.52	21.43±2.68
40.00	25.42±2.48	26.51±1.96	23.74±3.89	28.91±1.89	22.88±2.38	24.21±1.61
45.00	25.83±4.75	26.48±0.77	23.44±1.76	28.72±1.11	22.31±3.86	25.01±1.58
50.00	25.32±4.30	27.47±2.99	23.66±1.74	27.67±2.52	27.28±2.23	25.94±1.77
55.00	26.07±1.96	27.92±3.22	24.72±1.43	29.91±2.67	27.22±2.26	24.58±2.61
60.00	26.76±2.88	27.70±1.77	25.36±2.34	27.96±2.29	26.94±1.88	26.47±2.55
65.00	26.32±3.12	28.20±2.99	26.07±0.91	28.49±1.71	25.97±1.21	27.73±0.44
70.00	27.00±3.60	27.00±2.74	25.30±3.49	27.34±2.10	27.06±2.14	28.41±2.23
75.00	26.74±0.55	26.99±2.89	26.86±1.41	27.94±1.76	27.52±2.27	27.95±1.03

Notes:

- ***Rc**: recycled concrete aggregate / **Rb**:brick or clay-based material / **Ra:** asphalt/ **GL**: glass/ **PL**: plastic/ **W**: Wood*
- *± Standard deviation*

Table 6.Variations in the Ca/Si ratio in the ITZs

Distance from interface (μm)	Variation in Ca/Si ratio in ITZs					
	Rc	Rb	Ra	GL	PL	W
0	3.06±0.06	1.80±0.03	3.60±0.04	3.90±0.05	1.89±0.06	3.53±0.02
10	3.23±0.02	2.43±0.04	2.93±0.05	2.29±0.04	2.22±0.05	4.12±0.06
20	3.06±0.01	2.19±0.02	2.31±0.03	2.41±0.02	2.42±0.07	3.88±0.04
30	2.51±0.07	1.90±0.05	2.14±0.02	2.27±0.04	2.19±0.04	2.64±0.03
40	2.36±0.06	1.91±0.03	2.07±0.03	1.79±0.03	1.97±0.02	2.47±0.05
50	2.06±0.01	1.93±0.02	1.96±0.02	1.77±0.02	1.86±0.03	2.08±0.02
60	1.74±0.02	1.78±0.01	1.86±0.04	1.75±0.01	1.78±0.01	1.95±0.03
70	1.73±0.01	1.75±0.02	1.81±0.01	1.76±0.01	1.77±0.01	1.79±0.02
80	1.73±0.01	1.75±0.01	1.76±0.01	1.76±0.01	1.75±0.01	1.73±0.01
90	1.76±0.01	1.76±0.01	1.73±0.02	1.76±0.01	1.74±0.01	1.73±0.01
100	1.75±0.02	1.76±0.02	1.73±0.01	1.76±0.01	1.74±0.01	1.73±0.01

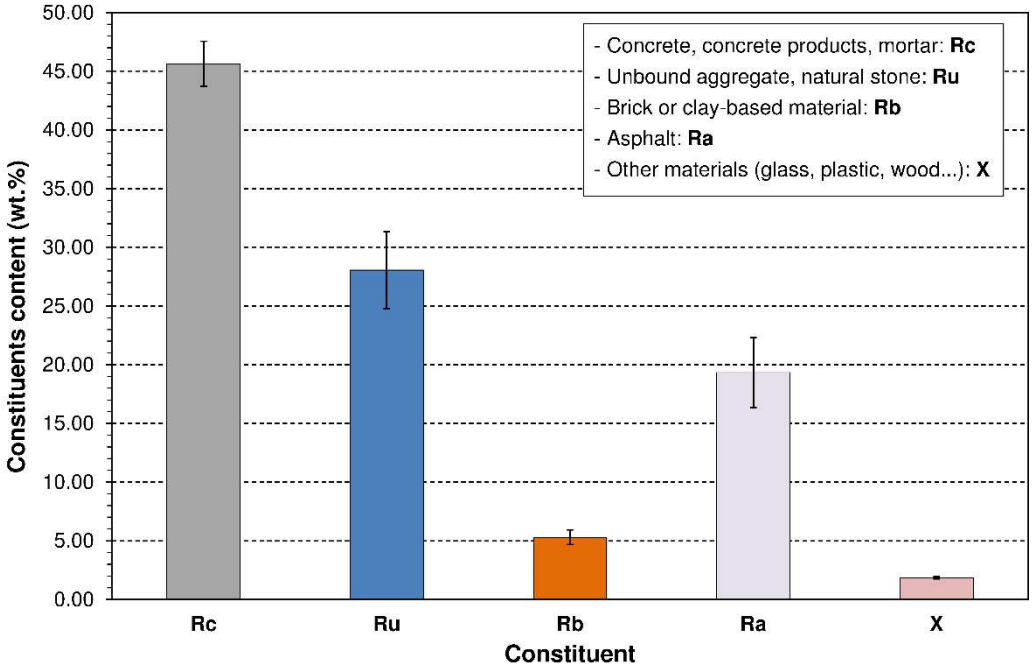

Figure 1. Composition of recycled mixed aggregate

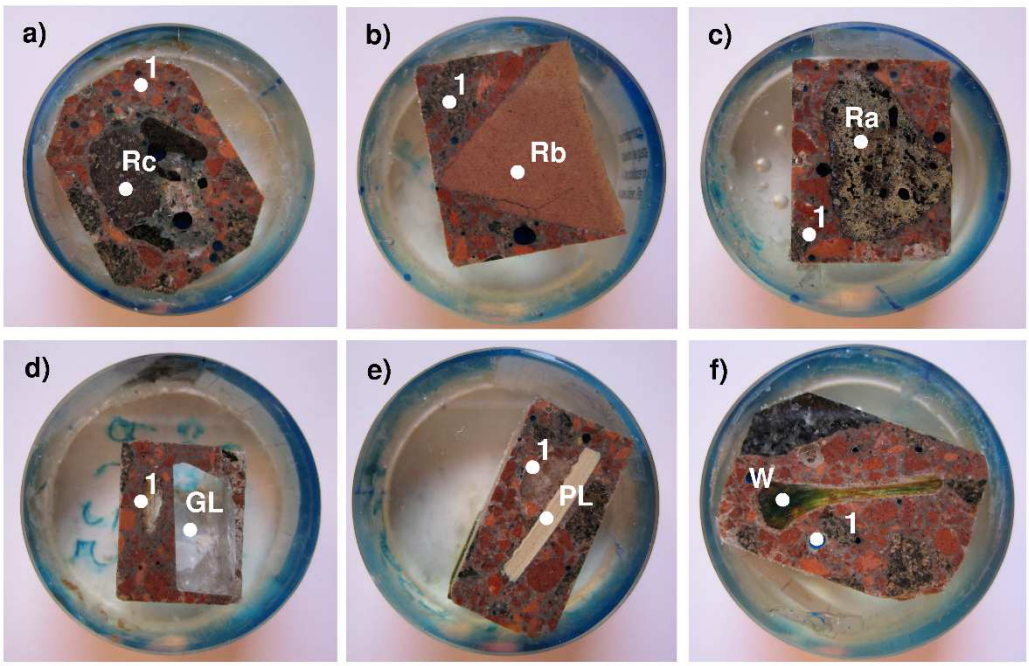

Figure 2. Indentation specimens: a) recycled concrete aggregate (RC)/paste; b) brick or clay-based material (Rb)/paste; c) asphalt (Ra)/paste; d) glass (GL)/paste; e) plastic (PL)/paste; f) wood (W)/paste

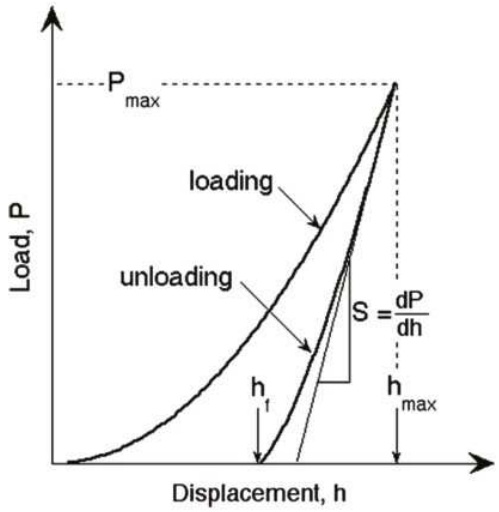

Figure 3. Indentation load vs. displacement curve obtained from nanoindentation/instrumented indentation testing

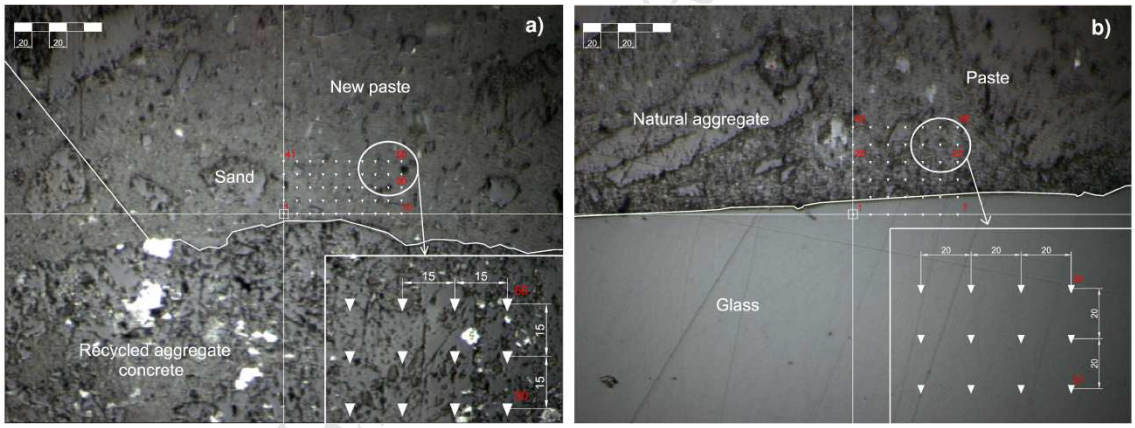

Figure 4. Area indented in recycled aggregate constituent/paste ITZ a) 15x15 μm; y b) 20x20 μm

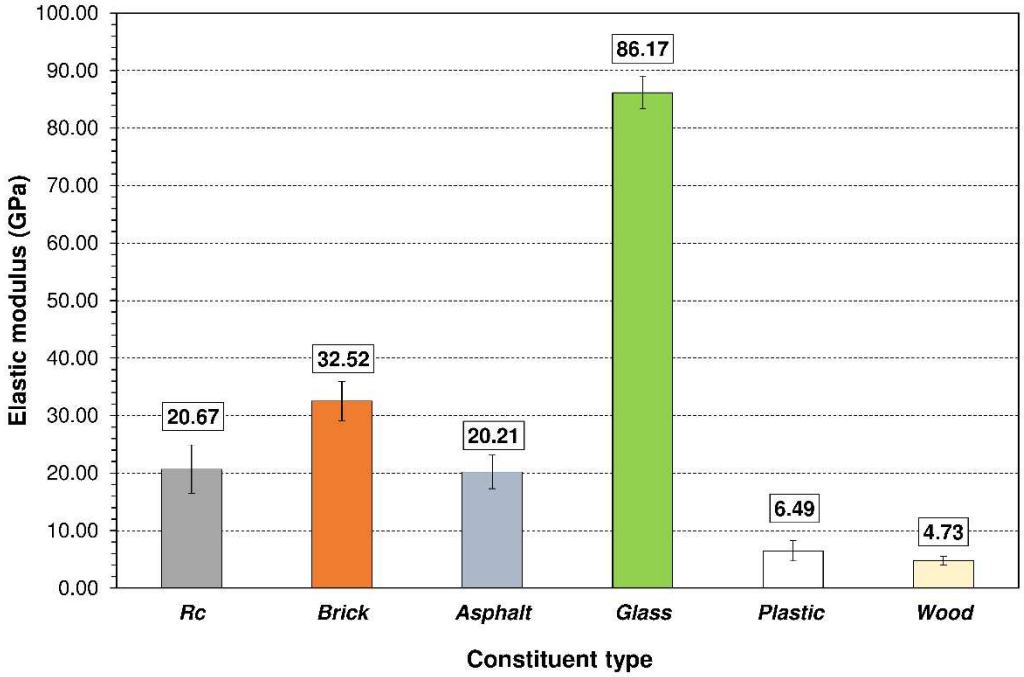

Figure 5. Nanoindentation-determined elastic modulus of recycled aggregate components

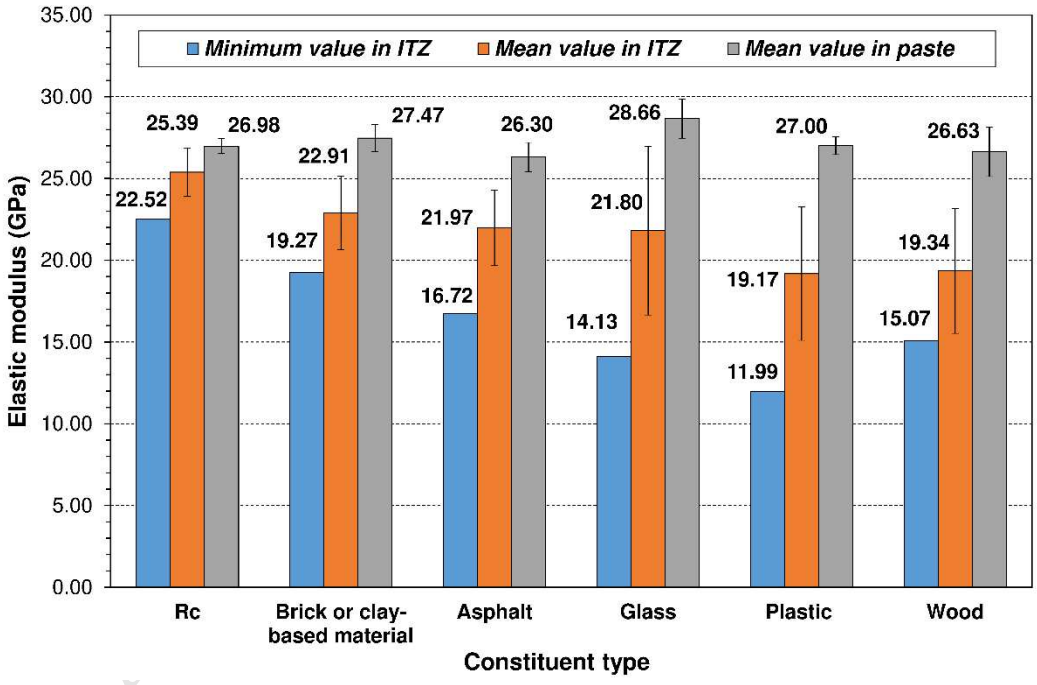

Figure 6. Minimum and mean elastic modulus (GPa) in the interfacial transition zone (ITZ) and mean value in paste

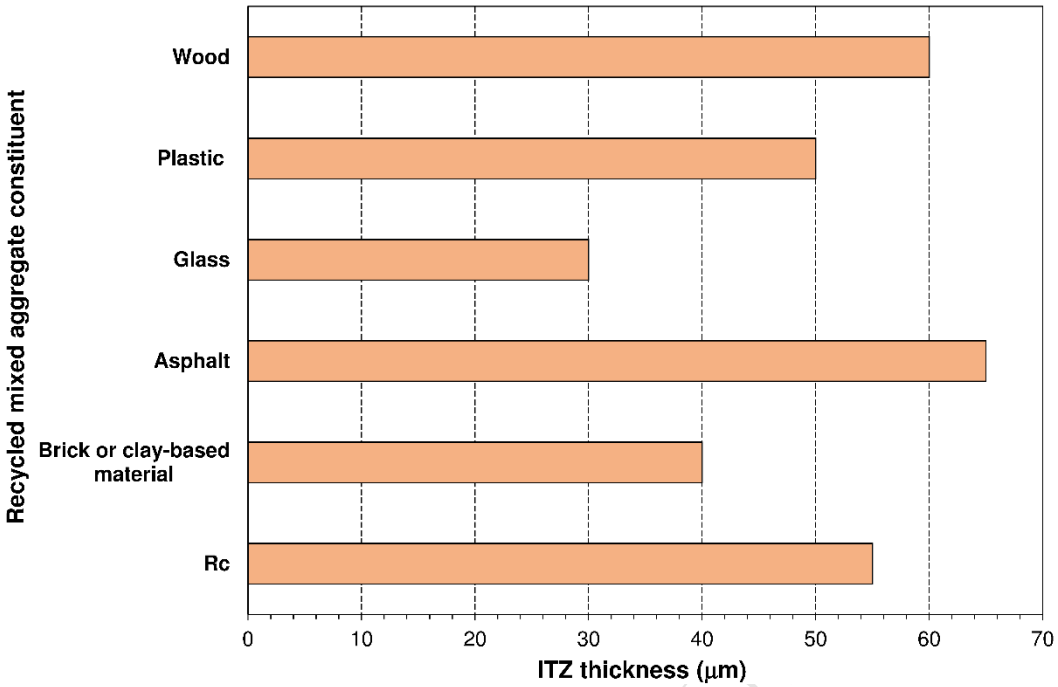

Figure 7. Nanoindentation-determined thickness of the recycled aggregate constituent/paste ITZ

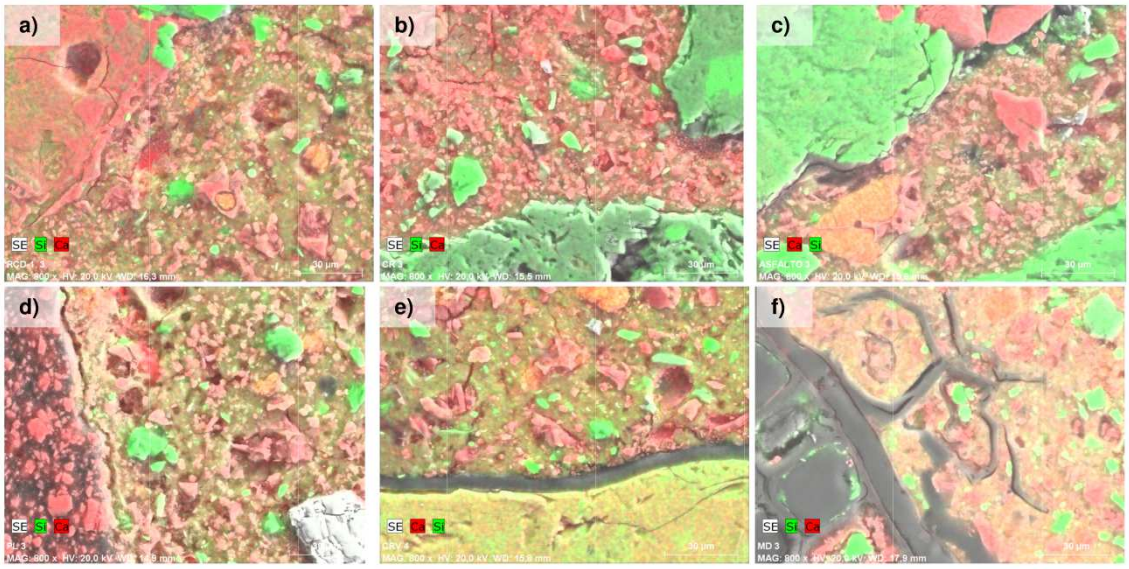

Figure 8. Microstructural analysis and Ca and Si mapping in ITZs: a) recycled concrete/paste; b) brick/paste; c) asphalt /paste; d) plastic/paste; e) glass/paste; f) wood/paste

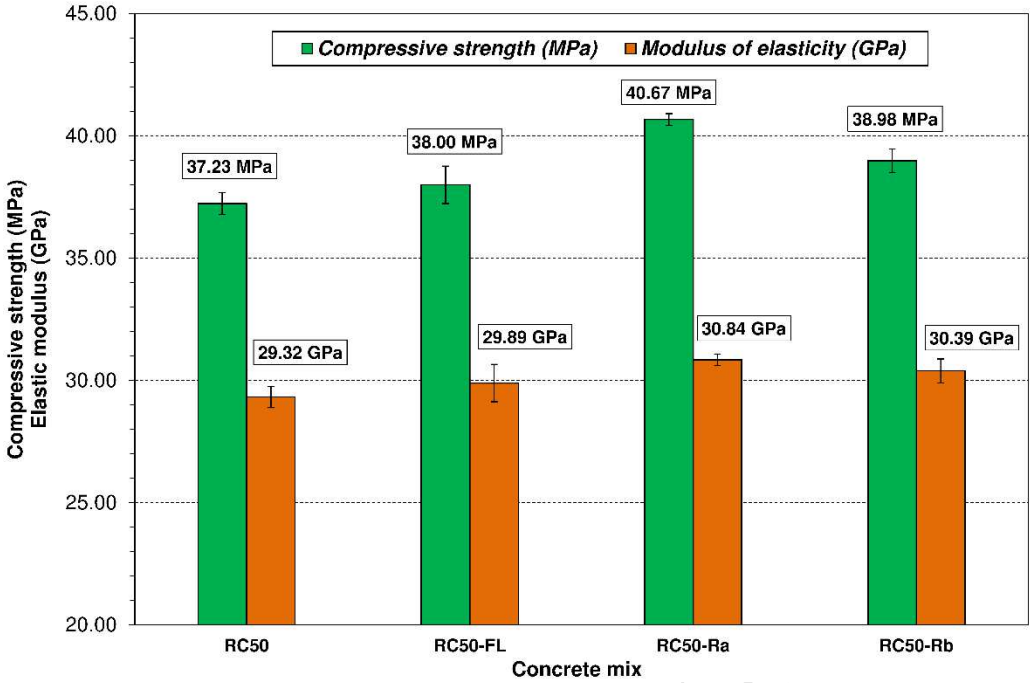

Figure 9. Macro-properties of 28-day concrete